Received: 14 March 2024 | Accepted: 11 May 2024

DOI: 10.1111/1759-7714.15381

ORIGINAL ARTICLE

WILEY

METTL3/IGF2BP1 influences the development of non-small-cell lung cancer by mediating m6A methylation modification of TRPV1

Wenjie Bai[1] | **Gang Xiao**[1,2] | **Guijing Xie**[1] | **Zhibo Chen**[1] | **Xie Xu**[1] | **Jie Zeng**[1] | **Jianjiang Xie**[1]

[1]Department of Thoracic Surgery, Guangzhou First People's Hospital, South China University of Technology, Guangzhou, China

[2]Center for Medical Research on Innovation and Translation, Guangzhou First People's Hospital, South China University of Technology, Guangzhou, China

Correspondence
Jianjiang Xie and Jie Zeng, Department of Thoracic Surgery, Guangzhou First People's Hospital, South China University of Technology, No. 1 Panfu Road, Guangzhou 510180, Guangdong, China.
Email: eyxiejianjiang@scut.edu.cn; eyzengjie@scut.edu.cn

Funding information
Guangzhou Municipal Science and Technology Project, Grant/Award Numbers: 202201010053, 2023A04J0622; Guangdong Basic and Applied Basic Research Foundation, Grant/Award Number: 2020A1515011290

Abstract

Background: Methyltransferase 3 (METTL3) accelerates N6-methyladenosine (m6A) modifications and affects cancer progression, including non-small-cell lung cancer (NSCLC). In this study, we aimed to explore the regulatory mechanisms of METTL3 underling NSCLC.

Methods: Immunohistochemical assay, quantitative real-time polymerase chain reaction (qRT-PCR) assay, and western blot assay were conducted for gene expression. MTT assay and colony formation assay were performed to explore cell proliferation capacity. Cell apoptosis and THP-1 cell polarization were estimated by flow cytometry analysis. Cell migration and invasion capacities were evaluated by transwell assay. Methylated RNA immunoprecipitation assay, dual-luciferase reporter assay, actinomycin D treatment and RIP assay were performed to analyze the relationships of METTL3, insulin-like growth factor 2 mRNA binding protein 1 (IGF2BP1), and transient receptor potential cation channel subfamily V member 1 (TRPV1). The functions of METTL3 and TRPV1 in vivo were investigated through establishing the murine xenograft model.

Results: TRPV1 expression was upregulated in NSCLC and related poor prognosis. TRPV1 silencing inhibited NSCLC cell growth and metastasis, induced NSCLC cell apoptosis, and repressed M2 macrophage polarization. The results showed that METTL3 and IGF2BP1 could regulate TRPV1 expression through m6A methylation modification. Moreover, METTL3 deficiency inhibited NSCLC cell growth, metastasis, and M2 macrophage polarization and facilitated NSCLC cell apoptosis, while TRPV1 overexpression restored the impacts. In addition, METTL3 knockdown restrained tumor growth in vivo via regulating TRPV1 expression.

Conclusion: METTL3 bound to IGF2BP1 and enhanced IGF2BP1's m6A recognition of TRPV1 mRNA, thereby promoting NSCLC cell growth and metastasis, and inhibiting M2 macrophage polarization.

KEYWORDS
IGF2BP1, METTL3, NSCLC, TRPV1

INTRODUCTION

Non-small-cell lung cancer (NSCLC) is the most common type of lung cancer, with genetic and cellular heterogeneity. The etiology of NSCLC is multifaceted and involves a

Wenjie Bai and Gang Xiao contribute to this work equally as co-first authors.

Jianjiang Xie and Jie Zeng contribute to this work equally as co-corresponding authors.

combination of genetic and environmental influences.[1,2] Current treatment options for NSCLC include surgery, chemotherapy, radiation, and targeted therapy.[3] Despite significant advances in the clinical diagnosis and treatment, NSCLC is often diagnosed at an advanced stage, which greatly reduces treatment options and leads to a bleak prognosis.[4,5] It is therefore essential to study the underlying mechanisms and search for possible biomarkers and new therapeutic targets for NSCLC.

The protein encoded by the transient receptor potential cation channel subfamily V member 1 (TRPV1) gene is the capsaicin receptor, a non-selective cation channel that can be activated by a variety of physical and chemical stimuli.[6,7] To date, TRPV1 has been identified to serve as an essential regulator in several tumor types, such as gastric cancer,[8] breast cancer,[9] and cervical cancer.[10] In NSCLC, TRPV1 was identified to aggravate tumor development.[11] Nonetheless, the exact roles and molecular mechanisms of TRPV1 in NSCLC are largely unexplored.

Methyltransferase 3 (METTL3) is a catalytic enzyme that plays an important role in mediating N6-methyladenosine (m6A) modification.[12] The importance of METTL3 in tumor progression has been extensively studied in recent years. For instance, METTL3 elevated LAMA3 expression via m6A modification to aggravate the malignancy of oral squamous cell carcinoma.[13] METTL3 promoted esophageal cancer development via mediating the m6A modification of EPPK1 and modulating PI3K/AKT pathway.[14] Moreover, METTL3 acted as a tumor promoter in NSCLC via m6A modification of SFRP2.[15] Even so, very little research on the underlying mechanisms of METTL3 in NSCLC has been done.

Insulin-like growth factor 2 mRNA binding protein 1 (IGF2BP1) works by targeting specific gene mRNAs to alter translation.[16] IGF2BP1 has been verified to play a promotional effect on NSCLC development.[17,18] TFAP4/IGF2BP1 exacerbated NSCLC development via m6A modification of TK1.[19] However, whether IGF2BP1 mediated TRPV1 expression in NSCLC was still unclear.

In this study, the functions and relations of TRPV1, METTL3, and IGF2BP1 in NSCLC development were investigated, with the aim of discovering novel therapy targets for NSCLC.

MATERIALS AND METHODS

Tissue samples

The clinical specimens (including tumor and adjacent non-tumor tissues) were harvested from NSCLC patients ($N = 36$) who accepted treatment at Guangzhou First People's Hospital, South China University of Technology. The procedures obtained approval from the Ethics Committee of Guangzhou First People's Hospital, South China University of Technology. Written informed consents were offered by the participants.

Immunohistochemical analysis

The formalin-fixed and paraffin-embedded tissues were cut into 4-μm sections, which were then dewaxed and hydrated with gradient ethanol. Next, the sections were incubated with blocking buffer for 5 min and incubated with primary antibodies against TRPV1 (Abcam), proliferating cell nuclear antigen (PCNA) (Abcam) or matrix metalloprotein 2 (MMP2) (Abcam) for 24 h followed by anti-secondary antibody (Abcam) incubation for 30 min. Next, the sections were colored using diaminobenzidine and counterstained using hematoxylin. The images were captured with microscope.

Cell culture

Human bronchial epithelioid cells (16HBE) were bought from Mingzhoubio. NSCLC cell lines (H1299 and A549) were bought from Procell. All cells were maintained in RPMI 1640 medium (Procell) supplemented with 10% FBS (Procell) and 1% penicillin–streptomycin (Procell) at 37°C in an incubator with 5% CO_2.

Cell transfection

To silence TRPV1, METTL3 or IGF2BP1 expression, short hairpin RNA (shRNA) against TRPV1, METTL3 or IGF2BP1 (sh-TRPV1, sh-METTL3 or sh-IGF2BP1) was transfected into NSCLC cells, and sh-NC transfected cells were used as control. To elevate IGF2BP1 or TRPV1, IGF2BP1 or TRPV1 overexpression vector (IGF2BP1 or TRPV1) was constructed and empty control pcDNA was used as control. The shRNAs and plasmids were provided by Ribobio and cell transfections were done by Lipofectamine 2000 (Invitrogen).

qRT-PCR

RNA extraction in tissues and cells was manipulated by TRIzol (Beyotime) and RNA concentration detection was done on a NanoDrop 2000 spectrophotometer. The RNAs were reversely transcribed into cDNAs using M-MLV Reverse Transcriptase Reagent (Promega). Quantitative real-time polymerase chain reaction (qRT-PCR) was executed with BeyoFast™ SYBR Green qPCR Mix (Beyotime) and gene expression was estimated with the $2^{-\Delta\Delta Ct}$ method. The used primers are exhibited in Table 1.

Western blot

By using RIPA buffer (Beyotime), RNAs in tissues and cells were extracted and examined with a BCA protein assay kit (Tiangen). The proteins were subjected to 10% SDS-PAGE

TABLE 1 Primer sequences used for qRT-PCR.

Name		Primers for PCR (5′–3′)
TRPV1	Forward	AGCGTTTGTCGACTGACTGA
	Reverse	AGCCTCCCATGAACCTTTCG
IGF2BP1	Forward	CTCTCGGAGGGGTTTCGGA
	Reverse	CTCTCGTTGAGGTTGCCGAT
METTL3	Forward	CAGAGGCAGCATTGTCTCCA
	Reverse	ATGGACACAGCATCAGTGGG
GAPDH	Forward	GGAGCGAGATCCCTCCAAAAT
	Reverse	GGCTGTTGTCATACTTCTCATGG

for electrophoresis and then blotted onto PVDF membranes. The proteins were blocked for 1 h using 5% skimmed milk and labeled overnight with primary antibodies against TRPV1, METTL3, IGF2BP1, and GAPDH. Subsequently, the proteins were probed for 2 h with HRP-bound secondary antibody. The bands were determined by ECL kit (Beyotime). The used antibodies were provided by Abcam.

MTT assay

H1299 cells and A549 cells were inoculated for 48 h in the 96-well plates and then 10 μL MTT (Solarbio) was added. After incubation for 4 h, DMSO (Solarbio) was supplemented to dissolve the formazans. The absorbance at 570 nm was measured.

Colony formation assay

1×10^3 H1299 and A549 cells were plated into six-well plates and then cultured for 14 days. The medium was changed every 3 days. Before observation, the cells were fixed using 4% paraformaldehyde (Solarbio) and dyed using 1% crystal violet (Solarbio).

Flow cytometry analysis

H1299 and A549 cells were re-suspended in binding buffer and dyed for 10 min using Annexin V-FITC and PI based on the instructions of Annexin V-FITC/PI Apoptosis Detection Reagent (Vazyme). Cell apoptosis was estimated with flow cytometry.

Transwell assay

The transwell insert chambers (Corning Incorporated) with or without Matrigel (Corning Incorporated) covered on the upper chamber were employed for cell invasion and migration analysis.

The cells in serum-free medium were appended into the top compartment and the culture medium was supplemented into the lower compartment. Following 24 h of incubation, the cells were fixed with 4% paraformaldehyde (Solarbio) and colored with 1% crystal violet (Solarbio). The invaded and migrated cells were photographed.

THP-1 cell polarization

THP-1 cells were planed seeded into six-well plates and then PMA (100 ng/mL; Solarbio) was added into complete media for 48 h of incubation to induce the maturation of macrophages. In the co-culture system, the pairing chambers were used. THP-1 cells and PMA were added into the lower chamber and the transfected NSCLC cells were inoculated into the top chamber. Finally, 18 h later, the ratio of CD163 + cells was analyzed using flow cytometry.

Methylated RNA immunoprecipitation assay

Magna MeRIP™ m6A reagent (Merck Millipore) was used for this experiment as previously described.[20]

Measurement of m6A modification

By using EpiQuik m6A RNA methylation quantitative reagent (Epigentek Group Inc.), TRPV1 m6A level was examined. Briefly, H1299 and A549 cells were transfected with sh-NC or sh-METTL3. The RNAs were extracted and then added with the assay hole with m6A standard, followed by the capture and TRPV1 antibody solution. After measuring the optical density value of each hole at 450 nm, m6A level was calculated through colorimetry and determined with a standard curve.

Dual-luciferase reporter assay

The wild-type or mutant (mut) sequences of TRPV1 containing or lacking m6A modification sites of METTL3 were cloned into pmirGLO plasmid (Promega) to generate the luciferase reporter vectors of TRPV1 and Mut-TRPV1. H1299 and A549 cells were co-transfected with sh-NC/sh-METTL3 and TRPV1/Mut-TRPV1 for 48 h of incubation. Dual-Luciferase Reporter Assay Reagent (Promega) was employed for luciferase intensity detection.

Actinomycin D treatment

H1299 cells with sh-NC, sh-METTL3 or sh-METTL3 + IGF2BP1 transfection were exposed to actinomycin D

(Act D; Sigma-Aldrich) at 0, 3, 6, and 9 h, then TRPV1 mRNA level was determined via qRT-PCR.

RIP assay

The experiment was conducted using Magna RIP RNA-Binding Protein Immunoprecipitation Reagent (Millipore). The extracts of sh-NC/sh-METTL3-transfected H1299 and A549 cells were cultured with RIP buffer containing magnetic beads conjugated to specific antibodies of IGF2BP1 (Abcam) or IgG (Abcam). TRPV1 enrichment in the isolated beads was determined.

Murine xenograft model

Sh-NC, sh-METTL3 or sh-METTL3 + TRPV1 was injected into BALB/c nude mice ($N = 6$ mice/group; Shanghai SLAC Laboratory Animals Co., Ltd.). Starting on day 8, the xenograft tumor size was examined every 3 days via (length×width^2)/2. Mice were sacrificed on day 23 and tumors were harvested for weight and other study. The experiments were authorized by the Ethics Committee of Animal Research of Guangzhou First People's Hospital, South China University of Technology.

Statistics analysis

GraphPad Prism 7 was adopted for the analysis of data from three independent experiments. Results were presented as mean ± standard deviation. The survival curve was obtained by a Kaplan–Meier plot and analyzed by the log-rank test. Difference analysis was executed by Student's *t*-test or one-way ANOVA. The linear relationship was analyzed by Spearman's correlation coefficient analysis, and $p < 0.05$ was thought to be significant.

RESULTS

TRPV1 was highly expressed in NSCLC tissues and cells

As predicted by The Cancer Genome Atlas (TCGA) database, TRPV1 expression was upregulated in lung adenocarcinoma (LUAD) (Figure 1a). Immunohistochemical (IHC) assay indicated that TRPV1 expression was higher in NSCLC tissues than normal tissues (Figure 1b). We detected the mRNA expression of TRPV1 in the collected NSCLC tissues ($N = 36$) and adjacent normal tissues. The results showed that TRPV1 was highly expressed in NSCLC tissues compared to normal tissues (Figure 1c). Moreover, the

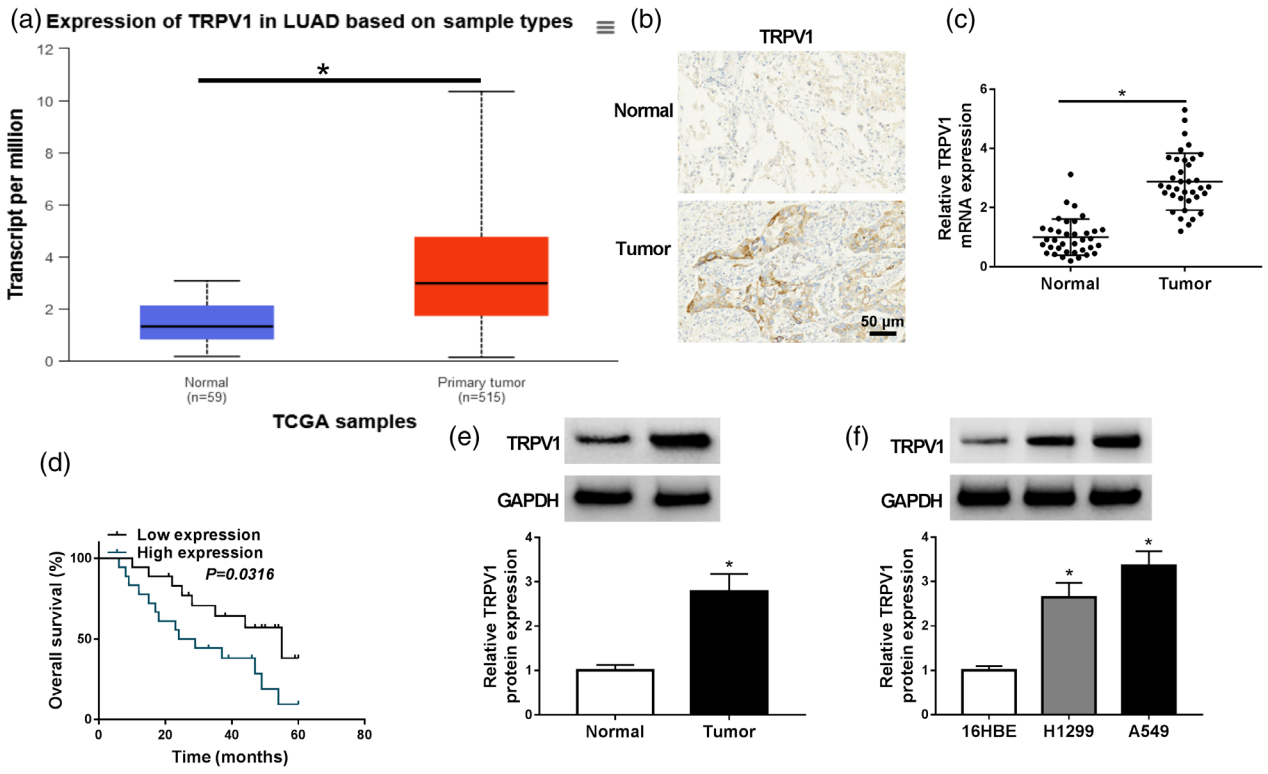

FIGURE 1 TRPV1 was upregulated in NSCLC tissues and cells. (a) TCGA database predicted TRPV1 expression in LUAD. (b) The expression of TRPV1 was estimated by immunohistochemical assay. (c) The mRNA expression of TRPV1 in NSCLC tissues and normal tissues was detected by quantitative real-time polymerase chain reaction (qRT-PCR). (d) The overall survival of NSCLC patients in the low expression group and the high expression group was analyzed. (e) The protein level of TRPV1 in NSCLC tissues and normal tissues was measured by western blot. (f) The TRPV1 protein level in human bronchial epithelioid cells, H1299, and A549 cells was measured through western blot. *$p < 0.05$.

NSCLC patients ($N = 36$) were divided into two groups according to TRPV1 expression: a low expression group and a high expression group. We found that the high expression of TRPV1 predicted worse overall survival compared to the low expression group (Figure 1d). Additionally, the TRPV1 protein level was elevated in NSCLC tissues in comparison with normal tissues (Figure 1e). Compared to 16HBE cells, the TRPV1 level was increased in H1299 cells and A549 cells (Figure 1f). Taken together, TRPV1 was abnormally elevated in NSCLC.

Silencing of TRPV1 hampered NSCLC cell proliferation, migration and invasion, and polarization of M2 macrophages.

To explore the functions of TRPV1 in NSCLC, sh-TRPV1 was introduced into NSCLC cells to silence TRPV1 expression. As shown in Figure 2a, sh-TRPV1 introduction markedly reduced the TRPV1 protein level in H1299 and A549 cells, indicating the successful introduction of sh-TRPV1. MTT assay suggested that the viability of H1299 and A549 cells was impeded by TRPV1 knockdown (Figure 2b). Similarly, TRPV1 deficiency led to the significant suppression of the colony formation of H1299 and A549 cells (Figure 2c). Flow cytometry analysis showed that TRPV1 silencing promoted the apoptosis of H1299 and A549 cells compared to the sh-NC control group (Figure 2d). As verified by transwell assay, knockdown of TRPV1 markedly repressed the migration and invasion of H1299 and A549 cells in comparison with sh-NC-transfected cells (Figure 2e,f). Additionally, sh-TRPV1 transfected H1299 and A549 cells reduced the ratio of $CD163^+$ cells, indicating that TRPV1 knockdown inhibited M2 macrophage polarization (Figure 2g). These findings illustrated that TRPV1 deficiency suppressed NSCLC cell growth and metastasis, promoted NSCLC cell apoptosis, and repressed M2 macrophage polarization.

Moreover, TRPV1 overexpression vector transfection elevated the TRPV1 level in H1299 and A549 cells compared to the pcDNA control group (Figure S1A). MTT assay and colony formation assay showed that the viability and colony

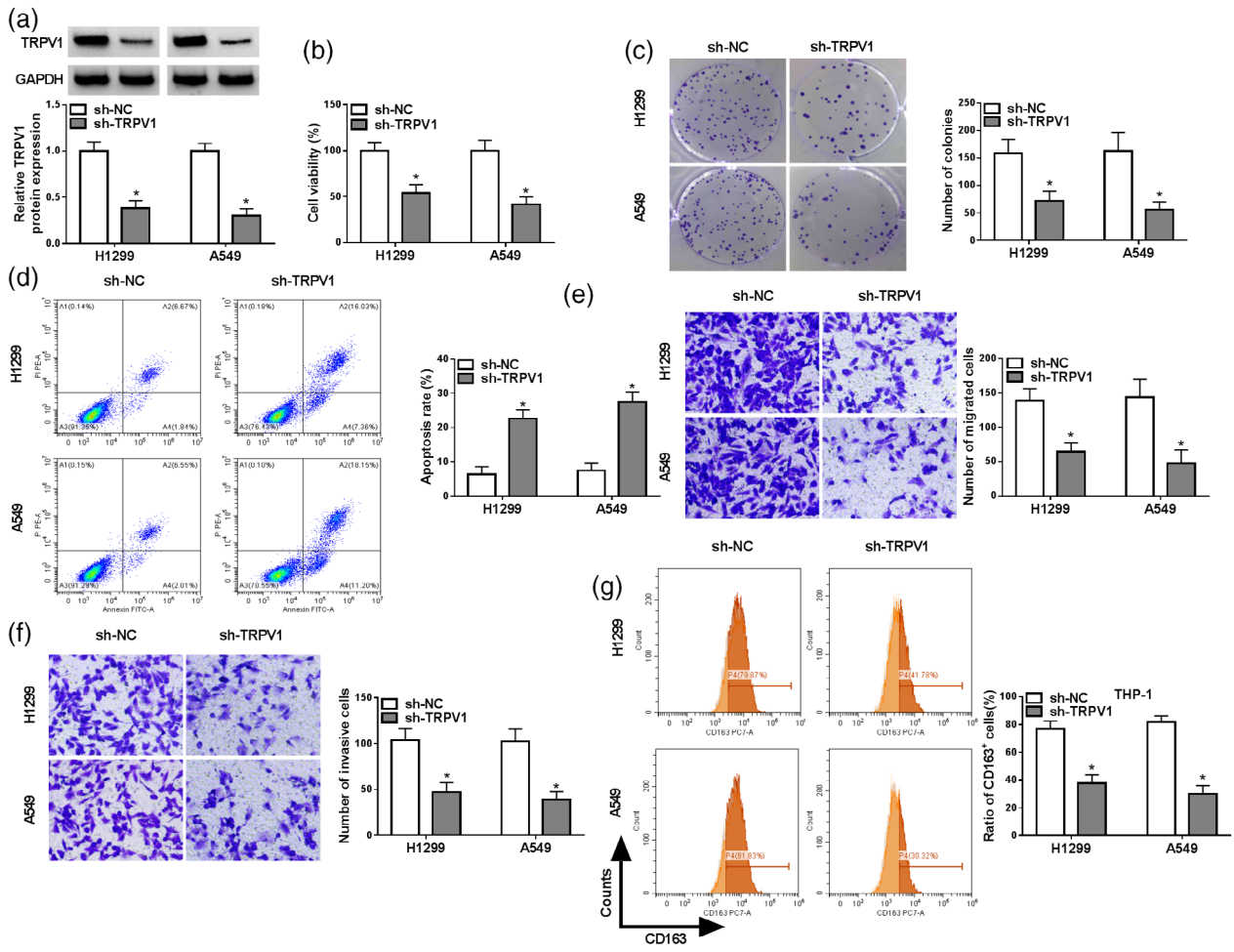

FIGURE 2 Effects of TRPV1 knockdown on NSCLC cell proliferation, apoptosis, migration, invasion, and M2 macrophage polarization. H1299 and A549 cells were transfected with sh-NC or sh-TRPV1. (a) The TRPV1 protein level in H1299 and A549 cells was measured through western blot. (b) H1299 and A549 cell viability was examined by MTT assay. (c) H1299 and A549 cell colony formation ability was tested by colony formation assay. (d) H1299 and A549 cell apoptosis was analyzed by flow cytometry analysis. (e and f) The migration and invasion of H1299 and A549 cells were explored by transwell assay. (G) The ratio of $CD163^+$ cells was analyzed by flow cytometry analysis. $^*p < 0.05$.

formation abilities of H1299 and A549 cells were promoted by TRPV1 overexpression (Figure S1B,C). Transwell assay showed that TRPV1 overexpression facilitated the migration and invasion of H1299 and A549 cells (Figure S1D,E). Additionally, TRPV1 overexpression promoted M2 macrophage polarization (Figure S1F). These results indicate that TRPV1 overexpression promoted NSCLC cell growth and metastasis and M2 macrophage polarization.

METTL3 mediated the m6A methylation modification of TRPV1

By using a methylated RNA immunoprecipitation assay, we precipitated the RNAs contained m6A methylation and found that TRPV1 was enriched in m6A methylation (Figure 3a). As presented in ENCORI and TCGA databases, TRPV1 was found to be positively correlated with METTL3 (Figure 3b,c). Moreover, te TCGA database showed that METTL3 was upregulated in LUAD tissues compared to normal tissues (Figure 3d). The qRT-PCR assay showed that the METTL3 mRNA level was increased in NSCLC tissues in comparison with normal tissues (Figure 3e). There was a positive correlation between the levels of METTL3 mRNA and TRPV1 mRNA in NSCLC tissues, as estimated by Spearman's correlation coefficient analysis (Figure 3f). Subsequently, sh-METTL3 was transfected into H1299 and A549 cells to knock down METTL3 expression, which was demonstrated by western blot (Figure 3g). METTL3 knockdown led to the reduction of TRPV1 mRNA expression in

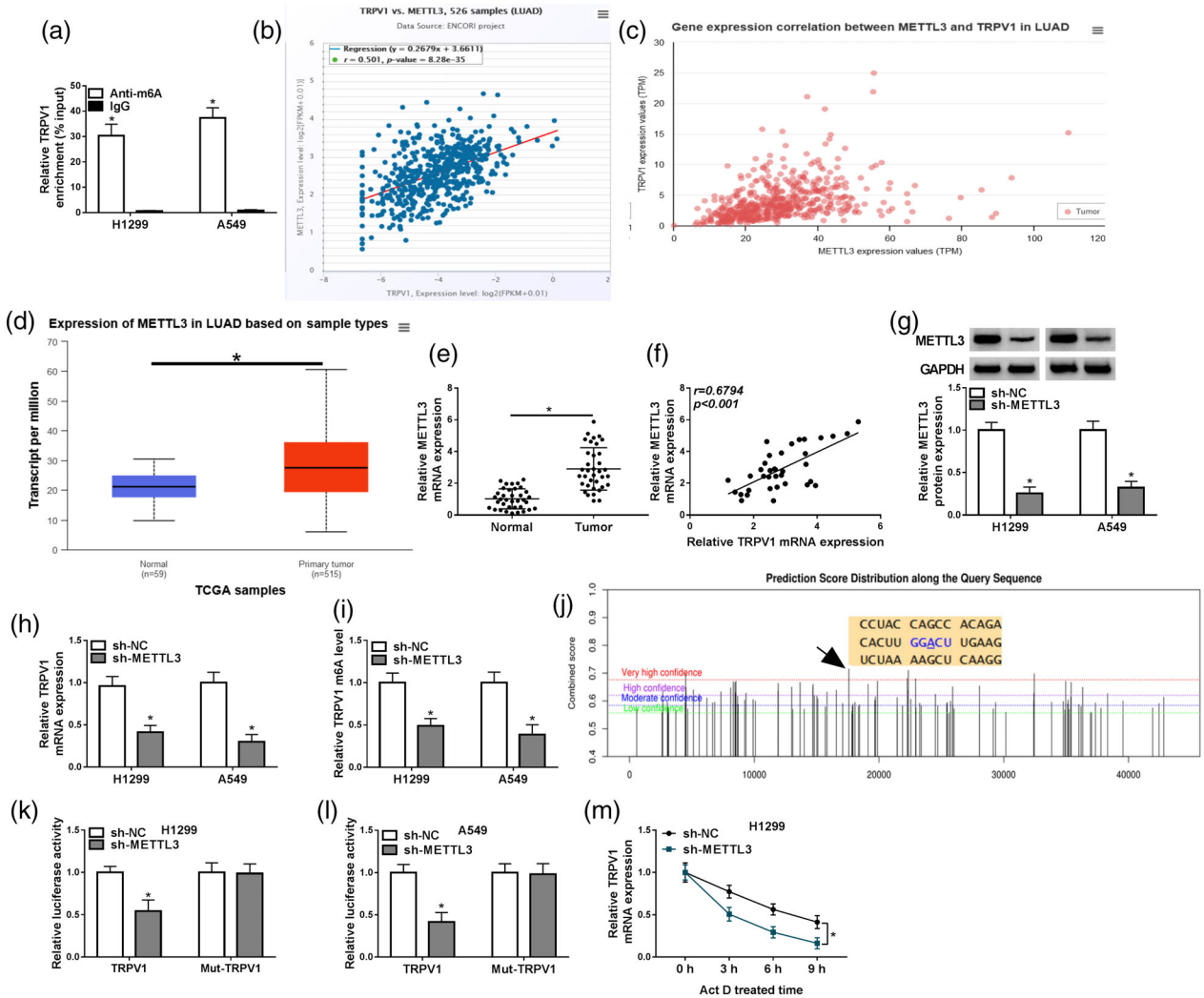

FIGURE 3 METTL3 modulated TRPV1 expression via m6A methylation modification. (a) After methylated RNA immunoprecipitation assay, TRPV1 enrichment was determined by qRT-PCR. (b and c) ENCORI and TCGA databases showed the positive correlation between the TRPV1 and METTL3 expression. (d) TCGA database showed that METTL3 was upregulated in LUAD. (e) The mRNA expression of METTL3 in NSCLC tissues and normal tissues was determined by qRT-PCR. (f) The correlation between the levels of METTL3 and TRPV1 in NSCLC tissues was analyzed by Spearman's correlation coefficient analysis. (g and h) After sh-NC or sh-METTL3 transfection, the METTL3 protein level and TRPV1 mRNA level in H1299 and A549 cells were determined by western blot and qRT-PCR, respectively. (i) THE TRPV1 m6A level in H1299 and A549 cells transfected with sh-NC or sh-METTL3 was examined. (j) SRAMP predicted TRPV1 mRNA contained m6A modification sites of METTL3. (k and l) The interaction relationship between METTL3 and TRPV1 was verified by dual-luciferase reporter assay. (m) After actinomycin D treatment for 0, 3, 6, and 9 h, TRPV1 expression in sh-NC or sh-METTL3-transfected H1299 cells was determined by qRT-PCR. $^*p < 0.05$.

H1299 and A549 cells (Figure 3h). Furthermore, we demonstrated that METTL3 knockdown reduced the TRPV1 m6A level in both H1299 and A549 cells (Figure 3i). According to the SRAMP website (http://www.cuilab.cn/sramp/), we found that the mRNA of TRPV1 contained m6A modification sites of METTL3 (Figure 3j). Dual-luciferase reporter assay showed that sh-METTL3 and TRPV1 co-transfection significantly restrained the luciferase activity in H1299 and A549 cells compared to sh-NC and TRPV1 co-transfected groups, but the luciferase activity in the Mut-TRPV1 group was not affected by sh-METTL3 (Figure 3k,l). In addition, Act D treatment showed that METTL3 knockdown repressed the stability of TRPV1 mRNA (Figure 3m). Collectively, METTL3 mediated m6A modification of TRPV1 to alter TRPV1 expression in NSCLC cells.

METTL3 bound to IGF2BP1 and enhanced the stability and expression of TRPV1 mRNA.

By detecting several methylated reading proteins (IGF2BP1, IGF2BP1, IGF2BP3, YTHDF1, YTHDF2, and YTHDF3), IGF2BP1 was found to affect TRPV1 expression (Figure 4a). RIP assay showed that METTL3 knockdown decreased the enrichment of IGF2BP1-bound TRPV1 in both H1299 and A549 cells, illustrating that METTL3 knockdown had an influence in the interaction between IGF2BP1 and TRPV1 (Figure 4b,c). Next, sh-IGF2BP1 and IGF2BP1 overexpression vector were transfected into H1299 and A549 cells to silence and enhance IGF2BP1 expression, and the results were demonstrated by western blot (Figure 4d). Act D treatment showed that METTL3 knockdown reduced TRPV1 expression in H1299 cells after Act D treatment, while IGF2BP1 overexpression reversed the effect (Figure 4e). Moreover, our results showed that METTL3 silencing decreased the TRPV1 protein level in H1299 and A549 cells, with IGF2BP1 overexpression ameliorating the impact (Figure 4f). Collectively, METTL3 bound to IGF2BP1 and enhanced IGF2BP1's m6A recognition of TRPV1 mRNA, thereby increasing the stability and expression of TRPV1 mRNA.

TRPV1 overexpression restored the effects of METTL3 knockdown on NSCLC cell proliferation, apoptosis, migration and invasion, and M2 macrophage polarization.

We further explored the relationship between METTL3 and TRPV1 in NSCLC malignant phenotype progression. As verified by western blot, METTL3 deficiency decreased the TRPV1 protein level in H1299 and A549 cells, while TRPV1 overexpression restored the impact (Figure 5a). MTT assay and colony formation assay demonstrated that METTL3 knockdown repressed the viability and colony formation

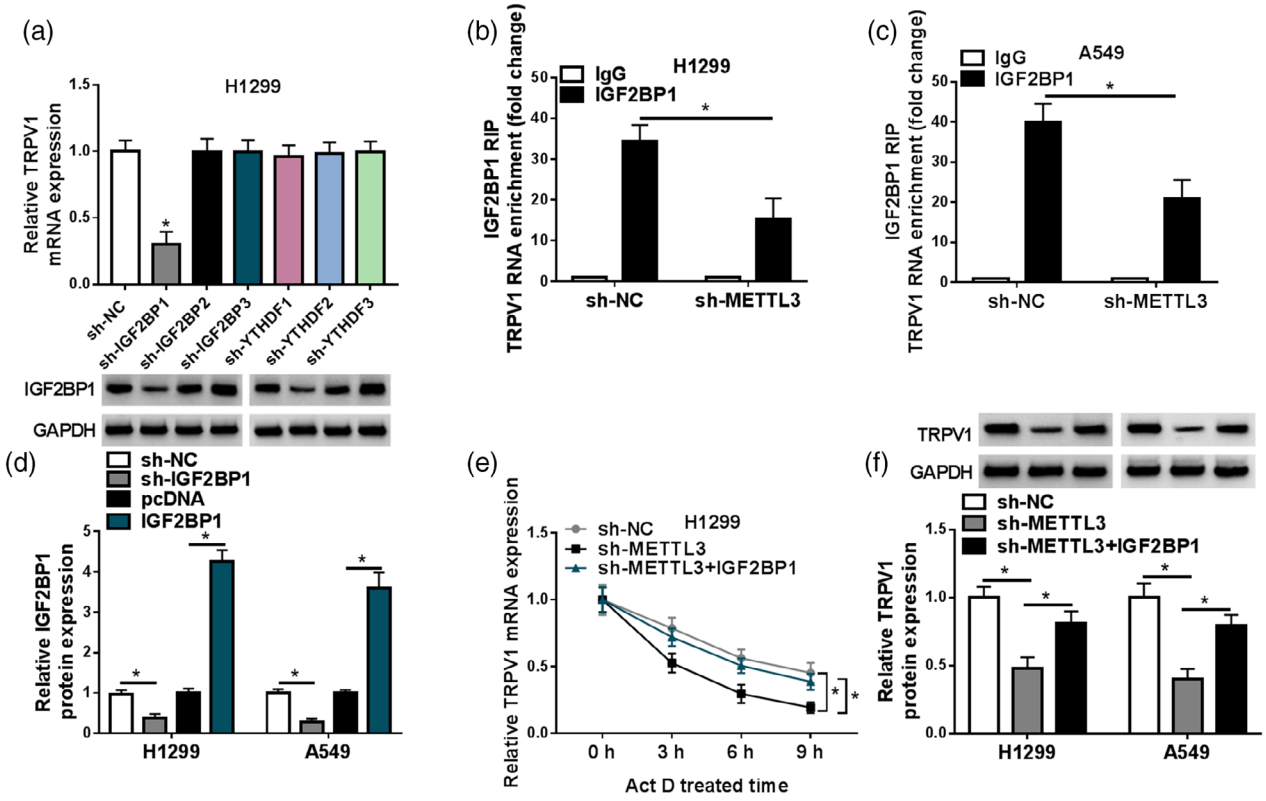

FIGURE 4 METTL3 bound to IGF2BP1 and enhanced the expression of TRPV1 mRNA. (a) TRPV1 mRNA expression in H1299 cells transfected with sh-NC, sh-IGF2BP1, sh-IGF2BP2, sh-IGF2BP3, sh-YTHDF1, sh-YTHDF2 or sh-YTHDF3 was determined by qRT-PCR. (b and c) The interaction between TRPV1 and IGF2BP1 was estimated by RIP assay in sh-NC or sh-METTL3 transfected H1299 cells. (d) After H1299 and A549 cells were transfected with sh-NC, sh-IGF2BP1, pcDNA or IGF2BP1, the TGF2BP1 protein level was measured by western blot. (e) After actinomycin D treatment for indicated times, TRPV1 mRNA level in H1299 cells transfected with sh-NC, sh-METTL3 or sh-METTL3 + TGF2BP1 was determined by qRT-PCR. (f) The protein expression of TRPV1 in H1299 and A549 cells transfected with sh-NC, sh-METTL3 or sh-METTL3 + TGF2BP1 was measured through western blot. $^*p < 0.05$.

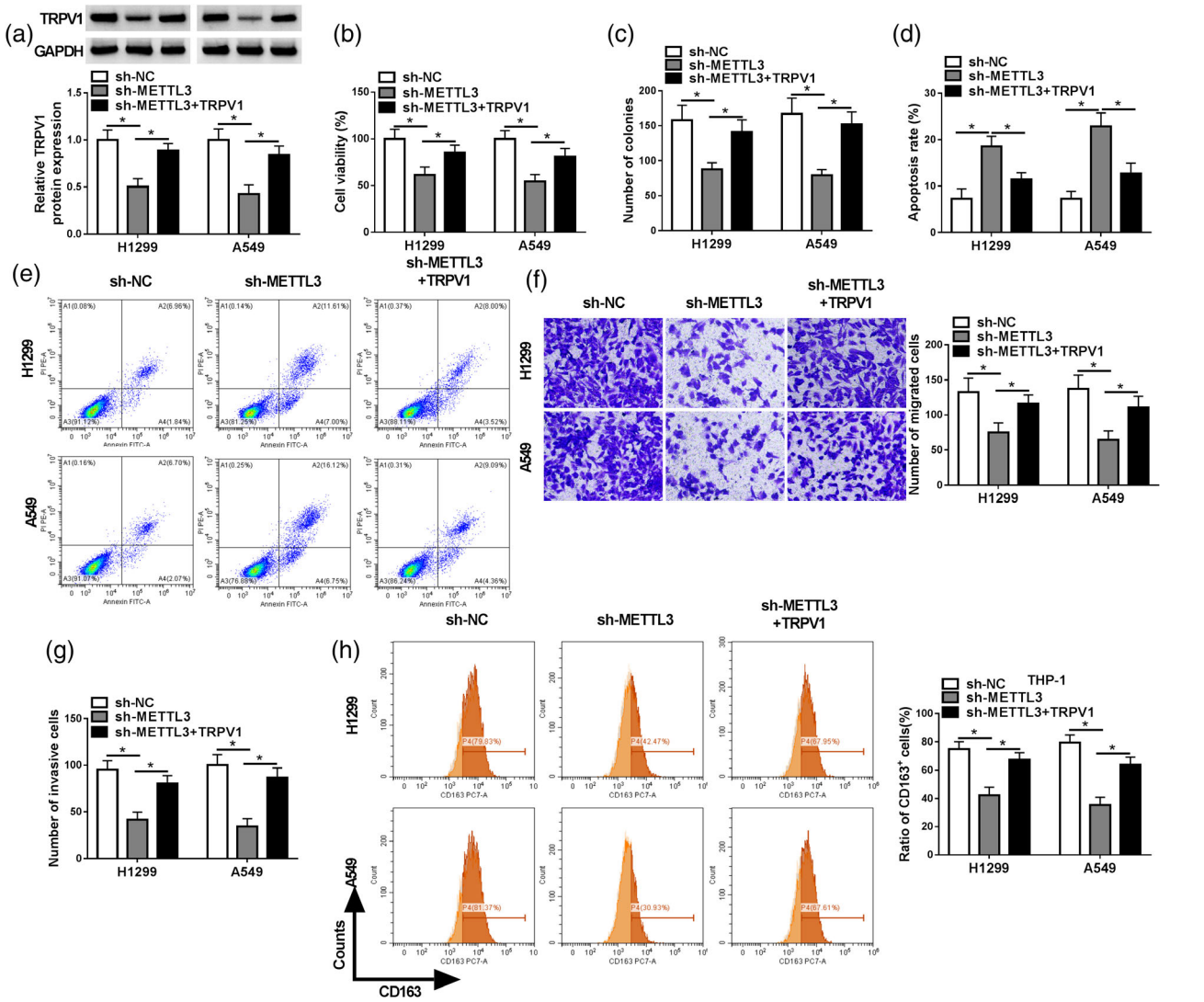

FIGURE 5 METTL3 knockdown repressed NSCLC cell growth, migration, and invasion and facilitated apoptosis and restrained M2 macrophage polarization. H1299 and A549 cells were transfected with sh-NC, sh-METTL3 or sh-METTL3 + TRPV1. (a) The protein level of TRPV1 in H1299 and A549 cells was measured via western blot. (b and c) The viability and colony formation of H1299 and A549 cells were estimated by MTT assay and colony formation assay, respectively. (d and e) The apoptosis of H1299 and A549 cells was analyzed by flow cytometry analysis. (f and g) The migration and invasion of H1299 and A549 cells were evaluated by transwell assay. (H) The ratio of $CD163^{+}$ cells was estimated through flow cytometry analysis. $^{*}p < 0.05$.

ability of H1299 and A549 cells, with TRPV1 enhancement ameliorating the effects (Figure 5b,c). As illustrated by flow cytometry analysis, METTL3 silencing facilitated H1299 and A549 cell apoptosis, whereas the effect was rescued by upregulating TRPV1 expression (Figure 5d,e). Transwell assay indicated that METTL3 silencing impeded the migration and invasion of H1299 and A549 cells, while TRPV1 overexpression abated the effects (Figure 5f,g). In addition, our results showed that METTL3 knockdown inhibited the polarization of M2 macrophages, but the impact was weakened by TRPV1 overexpression (Figure 5h). These outcomes suggested that METTL3 could modulate TRPV1 expression, thereby regulating NSCLC cell progression.

METTL3 knockdown repressed tumor growth in vivo via regulating TRPV1 expression.

Finally, the functions of METTL3 and TRPV1 in NSCLC progression were investigated by in vivo experiments. METTL3 knockdown suppressed the xenograft tumor growth (including tumor volume and weight), while TRPV1 overexpression partly restored the impacts (Figure 6a,b). We detected the expression of TRPV1 in the xenograft tumors. As a result, the TRPV1 protein level was reduced in the collected tumors in the sh-METTL3 group, while the TRPV1 level was reversed in the sh-METTL3 + TRPV1 group (Figure 6c,d). In addition, IHC assay showed that PCNA, MMP2, and TRPV1 expression in the tumors of the sh-METTL3 group was reduced, while their expression was restored in the sh-METTL3 + TRPV1 group (Figure 6e). Taken together, TRPV1 could reverse the inhibitory effect of METTL3 knockdown in tumor growth in vivo.

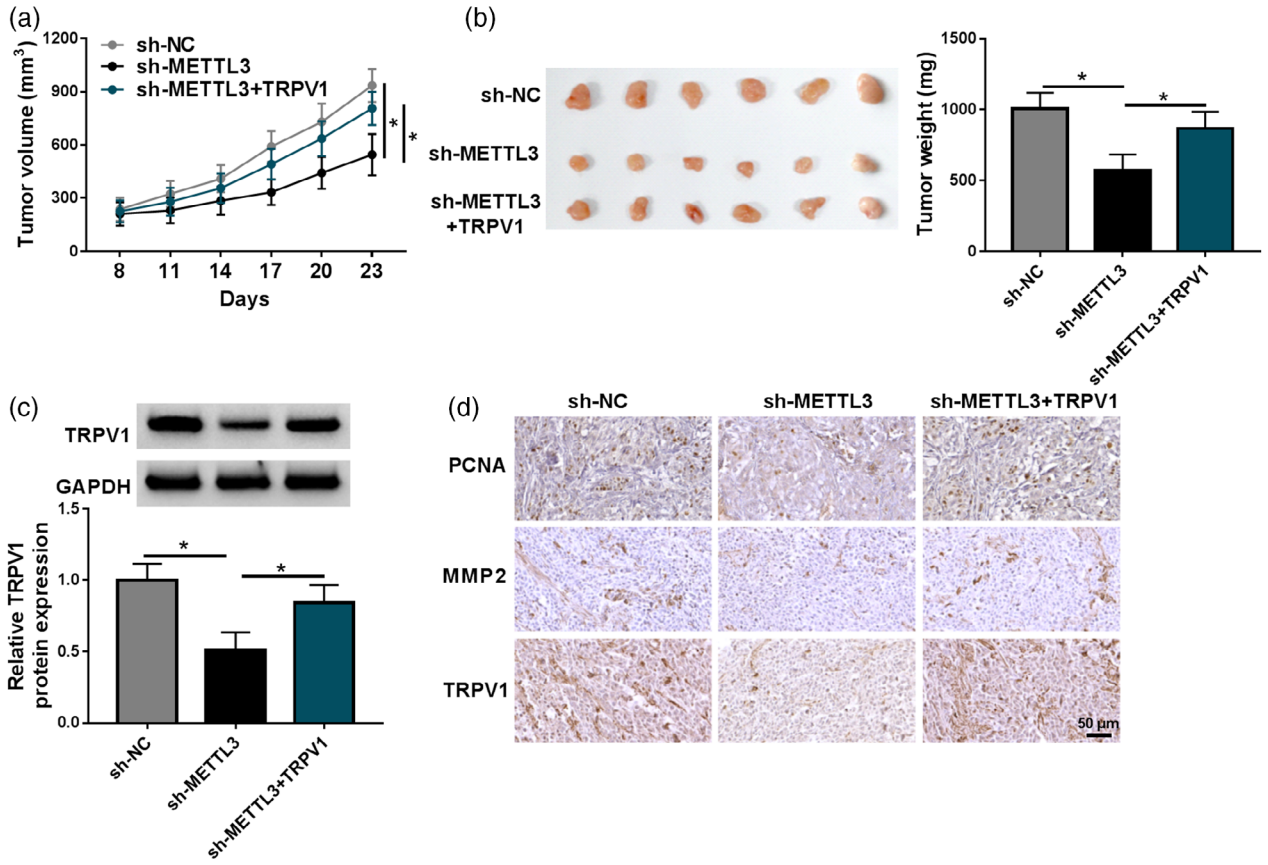

FIGURE 6 METTL3 regulated TRPV1 expression to affect tumor growth in vivo. (a) Tumor volume was monitored every 3 days after 8 days of sh-NC, sh-METTL3 or sh-METTL3 + TRPV1-transfected A549 cells introduction. (b) Tumor weight was examined after 23 days. (c and d) The TRPV1 protein level in the collected tumors was measured by western blot. (e) The expression of proliferating cell nuclear antigen (PCNA), matrix metalloprotein 2 (MMP2), and TRPV1 in the collected tumors was examined by immunohistochemical assay. $^*p < 0.05$.

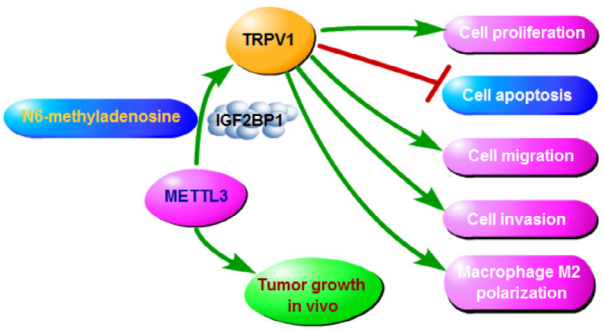

FIGURE 7 The overview diagram of METTL3/IGF2BP1-TRPV1 in NSCLC progression. METTL3 bound to IGF2BP1 and enhanced IGF2BP1's m6A recognition of TRPV1 mRNA, thereby promoting NSCLC cell proliferation, migration, invasion, and M2 polarization and inhibiting NSCLC apoptosis.

METTL3/IGF2BP1-mediated m6A modification of TRPV1 promoted NSCLC progression.

Through the above findings, we concluded that METTL3/IGF2BP1 mediated m6A methylation of TRPV1 to promote NSCLC cell proliferation, migration, and invasion, inhibited NSCLC cell apoptosis and facilitated macrophage M2 polarization (Figure 7).

DISCUSSION

The occurrence and development of NSCLC are closely related to epigenetic abnormalities, and m6A is a common and extremely important epigenetic change.[21] In the present research, METTL3, the key enzyme related to m6A methylation, was demonstrated to aggravate NSCLC malignancy and the METTL3/IGF2BP1–TRPV1 axis in NSCLC was discovered.

TRPV1 played vital roles in the development of multiple human cancers, including NSCLC. Wang et al. unrevealed that TRPV1 was aberrantly elevated in NSCLC and enhanced tumor growth and impeded the antitumor immune response.[11] Li et al. found that TRPV1 facilitated chemoresistance in NSCLC.[22] In this paper, high expression of TRPV1 in NSCLC was verified and predicted poor prognosis. Corresponding to the previous studies, TRPV1 deficiency impeded proliferation and motility, promoted the apoptosis of NSCLC cells, and repressed M2 macrophage polarization.

The involvement of m6A in various human cancers has attracted researchers' attention.[23,24] Thus, we further investigated whether the m6A modification of TRPV1 was related to NSCLC progression. By using the SRAMP website, it was

found that TRPV1 mRNA contained m6A modification sites of METTL3 and METTL3 positively altered TRPV1 expression. In NSCLC, METTL3 has been reported to act as a tumor promoter via the m6A methylation modifications of ZDHHC16,[25] SFRP2,[15] MALAT1,[26] and YTHDF1.[27] Moreover, previous studies demonstrated that METTL3 contributed to NSCLC cell metastasis and growth, and tumorigenesis.[28,29] Similarity, in the current study, METTL3 deficiency restrained NSCLC cell proliferation, metastasis, and M2 macrophage polarization and promoted NSCLC cell apoptosis, but the effects were restored by elevating TRPV1 expression. Additionally, METTL3 knockdown repressed tumorigenesis in vivo, with TRPV1 enhancement ameliorating the impact. Our findings illustrated that METTL3 played a tumor-promotional effect on NSCLC via modulating the m6A methylation modification of TRPV1.

Our results show that IGF2BP1 mediated METTL3 expression via m6A methylation modification. Xu et al. demonstrated that IGF2BP1 facilitated the migration, invasion, and proliferation of NSCLC cells.[30] Our study firstly investigated the relation between IGF2BP1 and METTL3, however, we did not explore the exact functions of IGF2BP1 and METTL3 in NSCLC.

In summary, METTL3/IGF2BP1 mediated TRPV1 expression via m6A methylation modification, thereby promoting NSCLC progression. This study provided an excellent basis for discovering novel therapeutic strategies for NSCLC.

CONFLICT OF INTEREST STATEMENT

The authors declare that they have no competing interests.

DATA AVAILABILITY STATEMENT

The analyzed data sets generated during the present study are available from the corresponding author on reasonable request.

CONSENT FOR PUBLICATION

Patients agreed to participate in this work.

ORCID

Jianjiang Xie https://orcid.org/0000-0002-8454-7753

REFERENCES

1. Chen Z, Fillmore CM, Hammerman PS, Kim CF, Wong KK. Non-small-cell lung cancers: a heterogeneous set of diseases. Nat Rev Cancer. 2014;14:535–46.
2. Sung H, Ferlay J, Siegel RL, Laversanne M, Soerjomataram I, Jemal A, et al. Global cancer statistics 2020: GLOBOCAN estimates of incidence and mortality worldwide for 36 cancers in 185 countries. CA Cancer J Clin. 2021;71:209–49.
3. Laface C, Maselli FM, Santoro AN, Iaia ML, Ambrogio F, Laterza M, et al. The resistance to EGFR-TKIs in non-small cell lung cancer: from molecular mechanisms to clinical application of new therapeutic strategies. Pharmaceutics. 2023;15:15.
4. Yu Y, He J. Molecular classification of non-small-cell lung cancer: diagnosis, individualized treatment, and prognosis. Front Med. 2013;7:157–71.
5. Tsao AS, Scagliotti GV, Bunn PA Jr, Carbone DP, Warren GW, Bai C, et al. Scientific advances in lung cancer 2015. J Thorac Oncol. 2016;11:613–38.
6. Caterina MJ, Schumacher MA, Tominaga M, Rosen TA, Levine JD, Julius D. The capsaicin receptor: a heat-activated ion channel in the pain pathway. Nature. 1997;389:816–24.
7. Jordt SE, Tominaga M, Julius D. Acid potentiation of the capsaicin receptor determined by a key extracellular site. Proc Natl Acad Sci USA. 2000;97:8134–9.
8. Deng R, Yu S, Ruan X, Liu H, Zong G, Cheng P, et al. Capsaicin orchestrates metastasis in gastric cancer via modulating expression of TRPV1 channels and driving gut microbiota disorder. Cell Commun Signal. 2023;21:364.
9. Okui T, Hiasa M, Hata K, et al. The acid-sensing nociceptor TRPV1 controls breast cancer progression in bone via regulating HGF secretion from sensory neurons. Res Sq. 2023. doi:10.21203/rs.3.rs-3105966/v1
10. Wang Z, Dong J, Tian W, Qiao S, Wang H. Role of TRPV1 ion channel in cervical squamous cell carcinoma genesis. Front Mol Biosci. 2022;9:980262.
11. Wang Y, Zhang Y, Ouyang J, Yi H, Wang S, Liu D, et al. TRPV1 inhibition suppresses non-small cell lung cancer progression by inhibiting tumour growth and enhancing the immune response. Cell Oncol (Dordr). 2023. doi:10.1007/s13402-023-00894-7
12. Liu J, Yue Y, Han D, Wang X, Fu Y, Zhang L, et al. A METTL3-METTL14 complex mediates mammalian nuclear RNA N6-adenosine methylation. Nat Chem Biol. 2014;10:93–5.
13. Ning B, Mei Y. LAMA3 promotes tumorigenesis of Oral squamous cell carcinoma by METTL3-mediated N6-Methyladenosine modification. Crit Rev Immunol. 2024;44:49–59.
14. Jia J, Yu L. METTL3-mediated m6A modification of EPPK1 to promote the development of esophageal cancer through regulating the PI3K/AKT pathway. Environ Toxicol. 2024;39:2830–41.
15. Zhao S, Song P, Zhou G, Zhang D, Hu Y. METTL3 promotes the malignancy of non-small cell lung cancer by N6-methyladenosine modifying SFRP2. Cancer Gene Ther. 2023;30:1094–104.
16. Jiang X, Liu B, Nie Z, Duan L, Xiong Q, Jin Z, et al. The role of m6A modification in the biological functions and diseases. Signal Transduct Target Ther. 2021;6:74.
17. Sun M, Wang L, Ge L, Xu D, Zhang R. IGF2BP1 facilitates non-small cell lung cancer progression by regulating the KIF2A-mediated Wnt/beta-catenin pathway. Funct Integr Genomics. 2023;24:4.
18. Zhang J, Luo W, Chi X, Zhang L, Ren Q, Wang H, et al. IGF2BP1 silencing inhibits proliferation and induces apoptosis of high glucose-induced non-small cell lung cancer cells by regulating Netrin-1. Arch Biochem Biophys. 2020;693:108581.
19. Shen Q, Xu Z, Sun G, Wang H, Zhang L. TFAP4 activates IGF2BP1 and promotes progression of non-small cell lung cancer by stabilizing TK1 expression through m6A modification. Mol Cancer Res. 2022;20:1763–75.
20. Meng W, Xiao H, Zhao R, Chen J, Wang Y, Mei P, et al. METTL3 drives NSCLC metastasis by enhancing CYP19A1 translation and oestrogen synthesis. Cell Biosci. 2024;14:10.
21. Qiu FS, He JQ, Zhong YS, Guo MY, Yu CH. Implications of m6A methylation and microbiota interaction in non-small cell lung cancer: from basics to therapeutics. Front Cell Infect Microbiol. 2022;12:972655.
22. Li L, Chen C, Xiang Q, Fan S, Xiao T, Chen Y, et al. Transient receptor potential Cation Channel subfamily V member 1 expression promotes chemoresistance in non-small-cell lung cancer. Front Oncol. 2022;12:773654.
23. Sun T, Wu R, Ming L. The role of m6A RNA methylation in cancer. Biomed Pharmacother. 2019;112:108613.
24. He L, Li H, Wu A, Peng Y, Shu G, Yin G. Functions of N6-methyladenosine and its role in cancer. Mol Cancer. 2019;18:176.
25. Liu Z, Jing C, Zhang W. METTL3-mediated m6A modification enhances ZDHHC16 expression in nonsmall- cell lung cancer patients, attenuating ferroptosis by suppressing CREB ubiquitination. Cell Mol Biol (Noisy-le-Grand). 2024;70:30–7.

26. Cao Y, Di X, Cong S, et al. RBM10 recruits METTL3 to induce N6-methyladenosine-MALAT1-dependent modification, inhibiting the invasion and migration of NSCLC. Life Sci. 2023;315:121359.
27. Dou X, Wang Z, Lu W, Miao L, Zhao Y. METTL3 promotes non-small cell lung cancer (NSCLC) cell proliferation and colony formation in a m6A-YTHDF1 dependent way. BMC Pulm Med. 2022; 22:324.
28. Qian S, Liu J, Liao W, Wang F. METTL3 promotes non-small-cell lung cancer growth and metastasis by inhibiting FDX1 through copper death-associated pri-miR-21-5p maturation. Epigenomics. 2023; 15:1237–55.
29. Liu C, Ren Q, Deng J, et al. c-MYC/METTL3/LINC01006 positive feedback loop promotes migration, invasion and proliferation of non-small cell lung cancer. Biom J. 2023;100664. doi:10.1016/j.bj.2023.100664
30. Xu Y, Xu L, Kong Y, Li K, Li J, Xu F, et al. IGF2BP1 enhances the stability of SIK2 mRNA through m(6)a modification to promote non-small cell lung cancer progression. Biochem Biophys Res Commun. 2023;684:149113.

SUPPORTING INFORMATION

Additional supporting information can be found online in the Supporting Information section at the end of this article.

How to cite this article: Bai W, Xiao G, Xie G, Chen Z, Xu X, Zeng J, et al. METTL3/IGF2BP1 influences the development of non-small-cell lung cancer by mediating m6A methylation modification of TRPV1. Thorac Cancer. 2024;15(26):1871–81. https://doi.org/10.1111/1759-7714.15381